2010

Enhanced dust heating in the bulges of early-type spiral galaxies

C Engelbracht

L Hunt

R Skibba

J Hinz

D Calzetti
University of Massachusetts - Amherst, calzetti@astro.umass.edu

Enhanced dust heating in the bulges of early-type spiral galaxies[*]

C. W. Engelbracht[1], L. K. Hunt[2], R. A. Skibba[1], J. L. Hinz[1], D. Calzetti[3], K. D. Gordon[4], H. Roussel[5], A. F. Crocker[3], K. A. Misselt[1], A. D. Bolatto[6], R. C. Kennicutt[7], P. N. Appleton[8], L. Armus[9], P. Beirão[9], B. R. Brandl[10], K. V. Croxall[11], D. A. Dale[12], B. T. Draine[13], G. Dumas[14], A. Gil de Paz[15], B. Groves[10], C.-N. Hao[16], B. D. Johnson[7], J. Koda[17], O. Krause[14], A. K. Leroy[18] [**], S. E. Meidt[14], E. J. Murphy[9], N. Rahman[19], H.-W. Rix[14], K. M. Sandstrom[14], M. Sauvage[20], E. Schinnerer[14], J.-D. T. Smith[11], S. Srinivasan[5], L. Vigroux[5], F. Walter[14], B. E. Warren[21], C. D. Wilson[19], M. G. Wolfire[6], and S. Zibetti[14]

(Affiliations can be found after the references)

Preprint online version: May 12, 2010

ABSTRACT

Stellar density and bar strength should affect the temperatures of the cool (T ~ 20 − 30 K) dust component in the inner regions of galaxies, which implies that the ratio of temperatures in the circumnuclear regions to the disk should depend on Hubble type. We investigate the differences between cool dust temperatures in the central 3 kpc and disk of 13 nearby galaxies by fitting models to measurements between 70 and 500 μm. We attempt to quantify temperature trends in nearby disk galaxies, with archival data from *Spitzer*/MIPS and new observations with *Herschel*/SPIRE, which were acquired during the first phases of the *Herschel* observations for the KINGFISH (key insights in nearby galaxies: a far-infrared survey with *Herschel*) sample. We fit single-temperature modified blackbodies to far-infrared and submillimeter measurements of the central and disk regions of galaxies to determine the temperature of the component(s) emitting at those wavelengths. We present the ratio of central-region-to-disk-temperatures of the cool dust component of 13 nearby galaxies as a function of morphological type. We find a significant temperature gradient in the cool dust component in all galaxies, with a mean center-to-disk temperature ratio of 1.15 ± 0.03. The cool dust temperatures in the central ~ 3 kpc of nearby galaxies are 23 (±3)% hotter for morphological types earlier than Sc, and only 9 (±3)% hotter for later types. The temperature ratio is also correlated with bar strength, with only strongly barred galaxies having a ratio over 1.2. The strong radiation field in the high stellar density of a galactic bulge tends to heat the cool dust component to higher temperatures, at least in early-type spirals with relatively large bulges, especially when paired with a strong bar.

Key words. Galaxies: ISM - Infrared: galaxies - Submillimeter: galaxies - dust, extinction

1. Introduction

The infrared emission from galaxies contains roughly half of the entire energy budget in the Universe (e.g., Hauser & Dwek 2001). In addition to providing information on the amount of attenuation suffered by the stellar light, the infrared emission provides clues to important physical quantities, such as the metal, dust, and cold gas content of galaxies (e.g., Draine et al. 2007, Bernard et al. 2008). Infrared spectral energy distributions (SEDs), especially those extending into the submillimeter regime, can be used to measure the dust mass and temperature in galaxies (e.g., Dunne et al. 2000, 2001; Seaquist et al. 2004; Vlahakis et al. 2005; Draine et al. 2007; Willmer et al. 2009; Liu et al. 2010).

These temperature measurements have shown that the dust is warmer in the centers of galaxies than in the outskirts (e.g., Alton et al. 1998; Radovich et al. 2001; Melo et al. 2002; Dupac et al. 2003). Cool dust at roughly the same temperature in spiral disks is detected *globally* at longer wavelengths (850 μm and 1.3 mm; Siebenmorgen et al. 1999; Dunne et al. 2000, 2001; Vlahakis et al. 2005), but there is also some evidence of a warmer temperature component associated with the central regions. Warmer dust temperatures tend to be associated with sig-

nificant star-formation activity, the resulting intense interstellar radiation field (Stevens et al. 2005) and the earlier Hubble type (Bendo et al. 2003).

Here we use the infrared SEDs, from 70 to 500 μm (a range which should be dominated by emission from grains in thermal equilibrium with the radiation field, e.g., Popescu et al. 2000, Engelbracht et al. 2008), of a local sample of 13 galaxies spanning the range of spiral galaxies in the Hubble sequence, to derive the temperature of the cool (T~ 20 − 30 K) dust component of the central region and the disks separately, and investigate differences in the dust heating in the two regions. To achieve this goal, we use the 250, 350, and 500 μm *Herschel*/SPIRE (Spectral and Photometric Imaging REceiver; Griffin et al. 2010) images of the galaxies combined with the *Spitzer*/MIPS (Multiband Imaging Photometer for *Spitzer*; Rieke et al. 2004) 70 and 160 μm images. Eventually we will use PACS (Photodetector Array Camera and Spectrometer; Poglitsch et al. 2010) imaging for this study, but at the time of this writing, the data were not yet available. These galaxies have little nuclear activity that might heat the dust, with only NGC 1097 having a strongly active nucleus, so this is the first study to cleanly separate the far-infrared properties of central and disk regions in a sample of normal galaxies.

Until recently, little work has been done to dissect the dust emission in galaxies into sub-galactic components, owing to the general paucity of infrared images with the required angular resolution and to poor long-wavelength sensitivity. Some recent

---

work includes a study of the galaxy pair NGC1512/1510 (a target also discussed in this paper), which finds that the dust temperature in the central region of NGC1512 is slightly higher than in the disk and that there is a significantly higher fraction of warm dust, in agreement with the center of NGC1512 being a starburst (Liu et al. 2010). Work by Muñoz-Mateos et al. (2009) examines radial trends in dust properties in a number of nearby galaxies.

The *Herschel* Space Telescope promises to yield a breakthrough in the study of subgalactic components in galaxies. This paper is the first investigation to leverage the longest wavelength *Herschel* data available for the KINGFISH (key insights on nearby galaxies: a far-infrared survey with *Herschel*; this program is largely derived from SINGS, the *Spitzer* infrared nearby galaxy survey by Kennicutt et al. 2003) sample of nearby galaxies, which will eventually total 61. Companion papers from the science demonstration phase for this program showcase the shorter wavelength imaging (Sandstrom et al. 2010) and the spectroscopic data (Beirão et al. 2010).

Here we present new SPIRE images acquired during the first few months of *Herschel* operations, in the context of the KINGFISH Open-Time Key Project. We divide each galaxy into two spatially-resolved zones: the circumnuclear region and the surrounding disk. Then we compare central temperatures with those for the disk.

2. Observations and data reduction

We observed 33 nearby galaxies with the SPIRE instrument on *Herschel* (Pilbratt et al. 2010) in the scan map mode as part of the KINGFISH program over the period of November 2009 to January 2010. They were observed in the scan mode out to 1.5 optical radii, to depths of (3.2, 2.5, and 2.9) mJy/beam at (250, 350, and 500) μm. They were reduced using the standard calibration products and algorithms available in HIPE (the *Herschel* Interactive Processing Environment; Ott 2010), version 1.2.5 or 2.0.0 (whichever version was the latest available when the target was observed, since the SPIRE calibration is not sensitive to this range of HIPE versions). We modified the offset-subtraction algorithm in the pipeline, by requiring it to measure the offset only outside bright objects in the field (usually the galaxy that we targeted)—this procedure reduced a small negative offset (6% in the first galaxy we observed, NGC 4559) in the background in the same rows and columns as the source to an undetectable level. Otherwise, the data reduction was performed using the default pipeline.

3. Analysis

Of the 33 galaxies observed, we selected 13 which had both a large extent (i.e., greater than several 160/500 μm beam diameters, or $\sim 2'$) and a bright disk (brighter than ~ 0.5 Jy at 500 μm, excluding the nucleus). These galaxies are listed in Table 1. For the wavelengths with significantly smaller beams (i.e., 70, 250, and 350 μm) than the largest used here, we convolved the data to the SPIRE 500 μm resolution using the kernels described by Gordon et al. (2008) and updated by those authors for *Herschel*. For each galaxy, we computed masks that isolated the disk and central regions. The outer mask is an ellipse sized to encompass the disk where it contrasts strongly with the background, at 1.2, 6.6, 2.7, 1.4, and 0.8 MJy/sr at 70, 160, 250, 350, and 500 μm (where the SPIRE data have been converted to MJy/sr as described below), respectively. The inner mask is a circle centered

Table 1. Galaxy sample and computed temperatures

Name	Hubble type	D^a (Mpc)	Spectral^b type	$T_{disk}{}^c$ (K)	$T_{center}{}^c$ (K)
NGC0628	SAc	7.3	HII?	22.7±0.4	24.2±0.5
NGC0925	SABd	9.0	HII	22.3±0.4	23.9±0.5
NGC1097	SBb	19.1	Sy1	23.4±0.5	28.7±0.7
NGC1291	SB0/a	10.4	…	18.3±0.3	27.6±0.6
NGC1512	SBa	14.4	HII	21.3±0.4	27.3±0.6
NGC3621	SAd	6.9	…	21.9±0.4	25.6±0.6
NGC4559	SABcd	8.5	HII	22.7±0.4	24.2±0.5
NGC4594	SAa	9.4	Sy1.9	21.3±0.4	22.9±0.4
NGC4631	SBd	7.6	HII	24.5±0.5	27.7±0.6
NGC5055	SAbc	10.2	Transition2	22.0±0.4	25.3±0.5
NGC5457	SABcd	7.1	HII	23.4±0.5	23.9±0.5
NGC6946	SABcd	6.8	HII	24.5±0.5	26.6±0.6
NGC7331	SAb	14.9	Transition2	23.2±0.4	26.2±0.6

^{a} As listed in NED: The NASA/IPAC Extragalactic Database (NED) is operated by the Jet Propulsion Laboratory, California Institute of Technology, under contract with the National Aeronautics and Space Administration.
^{b} from NED or Ho et al. 1997
^{c} includes uncertainty in the photometric calibration

on the galaxy peak, with a minimum size chosen to be as small as possible (i.e., set by the MIPS 160 μm beam) and with a radius inversely proportional to the distance to the galaxy. Thus, a similar physical region of ~ 3 kpc diameter (in which one would expect to find structures like a bulge, bar, ring, and/or inner disk, e.g., see Erwin & Sparke 2002, Athanassoula & Martinet 1980, and Knapen 2005) is sampled in the central region of each galaxy. Our results are not sensitive to a modest change in the aperture size, for example, similar results are achieved with a fixed central aperture size of 40″ for each galaxy. A sample mask is shown in Fig. 1.

We measured flux densities in these apertures for each of the 3 *Herschel*/SPIRE bands, as well as the *Spitzer*/MIPS 70 and 160 μm bands. The *Herschel*/SPIRE data were calibrated in units of Jy/beam, which we converted to Jy by assuming beam sizes of 371, 720, and 1543 square arcseconds in the 250, 350, and 500 μm bands, respectively (Swinyard et al. 2010). We assign uncertainties as the quadratic sum of the data-dependent scatter and (by far the larger term) the uncertainty in the absolute calibration, taken to be 5% and 12% for *Spitzer*/MIPS at 70 and 160 μm (Gordon et al. 2007 and Stansberry et al. 2007, respectively) and 16% (the quadratic sum of the 15% absolute calibration uncertainty from Swinyard et al. 2010 and a 2% uncertainty in the size of the beam) for SPIRE data.

To each set of data, we fit a blackbody with a frequency-dependent emissivity of 1.5. Our conclusions do not change if values of 1 or 2 are used, although the temperatures increase or decrease, respectively. The uncertainties in the temperatures were computed via a Monte Carlo simulation, in which we performed 10000 trials where the photometric measurements were allowed to vary in a normal distribution with a standard deviation indicated by the photometric uncertainty. An example of fits and data points is shown in Fig. 2, where we can see that the 250 μm flux density is underpredicted by this simple model. This happens frequently in our dataset, and may be a sign that multiple temperature components are present in the regions we measured. The values of the *Herschel*/SPIRE uncertainty indicated by the uncertainty in the absolute calibration were allowed to vary together; i.e., the calibration uncertainty was assumed to be correlated among the three bands. In contrast, we allowed the MIPS uncertainties to vary independently; while not being strictly in-
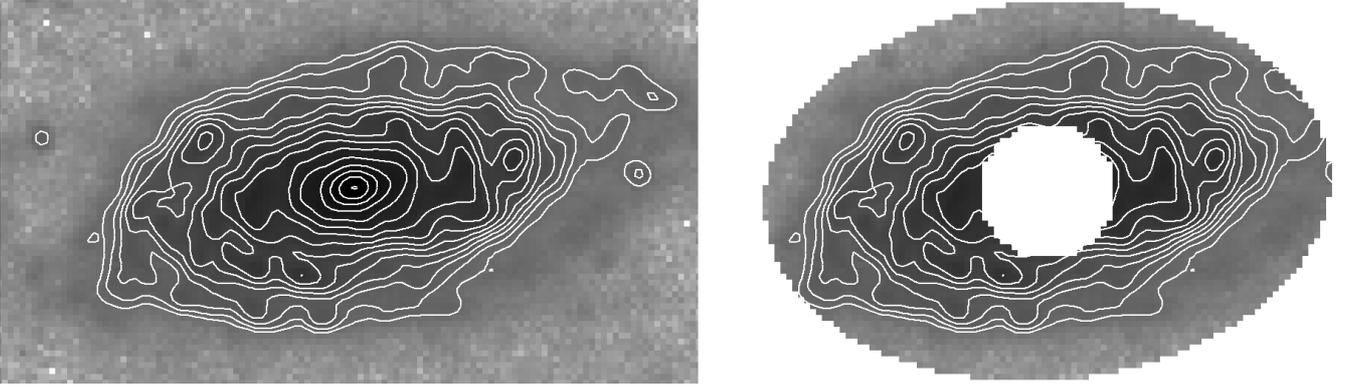
Fig. 1. Example of the masking approach used, shown here at 250 μm on a cropped image of NGC 5055. The image on the left shows the full, reduced image, while to the image on the right we have applied a mask (the blank, white regions) to all data but the disk. Both images have been scaled logarithmically, from -0.01 to 5 Jy/beam. The contour levels are scaled logarithmically from 0.1 to 5 Jy/beam. Each panel is 6′ across.
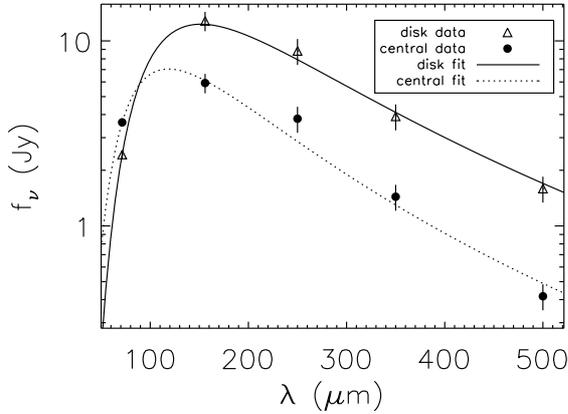

Fig. 2. Far-infrared SEDs of the disk and central region of NGC 1512, each fit by a blackbody function modified by a $\lambda^{-1.5}$ emissivity.
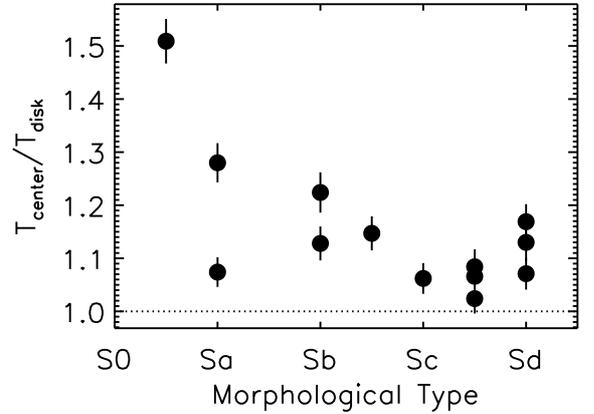

Fig. 3. Ratio of central dust temperature to disk dust temperature as a function of morphological type. The dotted line is drawn at a ratio of 1 (i.e., at equal temperatures) to guide the eye.
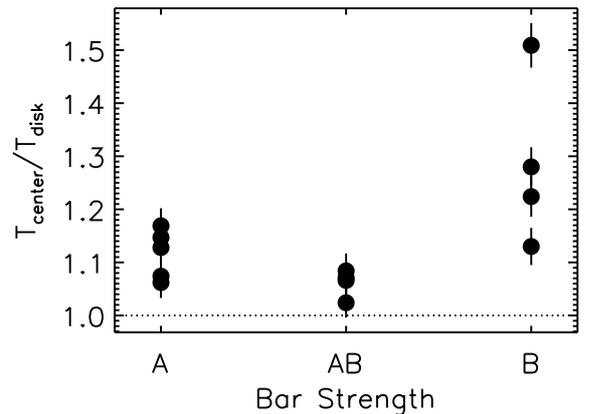
dependent (see Stansberry et al. 2007), the 160 μm calibration observations, in particular, are dominated by observational scatter and can be treated independently of the 70 μm band. The temperature of each component is taken to be the temperature of the best-fit model, with an uncertainty determined by the Monte Carlo simulation.

4. Results

For each galaxy, we computed a ratio of the central to disk temperature (from data at wavelengths longer than 70 μm) of the cool dust component. The average ratio of central-to-disk temperatures in this sample is 1.15 ± 0.03. We have plotted this ratio against morphological type in Figure 3, where the average ratio is 1.23 ± 0.03 for types earlier than Sc and 1.09 ± 0.03 for later types. The trend is poorly described by a line, because it has a correlation coefficient of 0.66. We plot the ratio against bar strength (as defined by the morphological type) in Fig. 4, where the average ratio is 1.29 ± 0.04 for strong bars and 1.09 ± 0.03 for weak bars.

A significant (3σ) correlation between temperature ratio and Hubble type is observed in Fig. 3, although the correlation is

Fig. 4. Ratio of central dust temperature to disk dust temperature as a function of bar strength, as indicated by morphological type. The dotted line is drawn at a ratio of 1 (i.e., at equal temperatures) to guide the eye.

only marginal, at 2σ, if the most significant point (NGC 1291) is removed from the correlation. This trend suggests that the dominant stellar bulges in early-type spirals are able to heat the cool dust in the ISM to greater temperatures than their late-type counterparts. The effect is most pronounced in the earliest type galaxy in our sample, NGC 1291, in which the dust in the central region is almost 50% warmer than the dust in the disk. In comparing this to the spectral types in Table 1, we have found no obvious correlation between the temperature ratio and the presence of a central nonthermal source in our galaxies.

Bars may play an important role in driving the correlation of temperature ratio with morphology. As shown in Fig. 4, a strong bar is correlated with a high center/disk temperature ratio, although the scatter in the strong-bar ratios is large. This could occur through bar-induced starbursts, since mid-infrared colors are redder in barred galaxies, implying warmer dust temperatures (Huang et al. 1996; Roussel et al. 2001). Barred galaxies also tend to have higher star-formation rates (SFRs) than unbarred galaxies, possibly because bars drive gas into the inner regions where it can pile up in the inner dynamical resonances associated with rings (Hawarden et al. 1986). The bar-driven gas transport has been shown in CO observations (e.g., Sakamoto et al. 1999). Stars will form quite readily in such conditions, where the gas transported by the bar fuels star formation (Erwin & Sparke 2002; Böker et al. 2008; Comerón et al. 2008). In fact, the frequency of inner rings in early-type barred spirals (Hunt & Malkan 1999; Erwin & Sparke 2002) could conspire to produce the effect seen in our sample. Similarly, bars are more frequently found in bulge-dominated galaxies (e.g., Masters et al. 2010), which would also contribute to the trends we see. The concentrations of CO gas in the centers have been observed in early-type spiral galaxies with intense star formation (Koda et al. 2005). In addition to a dependence on stellar density, the higher temperature ratios in the early types shown here could therefore be associated with bar-induced star formation. This is consistent with the result we get if the $70\,\mu$m fluxes are not included in the modified blackbody fits. Without them, the correlation between temperature ratio and either Hubble type or bar strength disappears; i.e., measurements at wavelengths shorter than the peak emission are required to determine the dust temperature accurately.

5. Conclusion

We used far-infrared data from *Spitzer* and submillimeter data from *Herschel* to compute separate SEDs for the center and disk regions of 13 nearby galaxies observed as part of the KINGFISH program. We fit those SEDs (at wavelengths longer than $70\,\mu$m) with blackbody functions (modified by a frequency-dependent emissivity) to compute temperatures. On average, the cool dust temperature of the central component is 15 ± 3% hotter than the disk. We find that the central temperature is higher than the disk by 20% to 50% in galaxies of type S0 to Sb, but only 9% higher in later types. This ratio is also higher (at 1.29 ± 0.04) in strongly barred galaxies than in weakly barred galaxies (at 1.09 ± 0.03).

The data therefore indicate that the large (or "classical") grains that dominate the far-infrared and submillimeter emission are warmer in the centers of those galaxies with a substantial bulge and/or a strong bar. This may simply be caused by the higher density of the radiation field in the centers of early-type spirals, enhanced star formation due to the bar, or some combination of the two. A cleaner separation of morphological components (perhaps with larger samples and/or less distant galaxies) and a more thorough assessment of the density of starlight and star formation activity, plus an evaluation of the impact of central nonthermal sources, may help separate these effects.

The analysis presented here illustrates the power of *Herschel* observations in characterizating the spatially resolved distribution of dust in nearby galaxies. This power will grow with the use of better-resolved far-infrared SEDs as measured by PACS (Poglitsch et al. 2010), which will let us measure smaller and/or more distant galaxies and determine radial trends of dust temperature.

References

Alton, P. B., et al. 1998, A&A, 335, 807
Athanassoula, E., & Martinet, L. 1980, A&A, 87, L10
Beirão, et al. 2010, this volume
Bendo, G. J., et al. 2003, AJ, 125, 2361
Bernard, J.-P., et al. 2008, AJ, 136, 919
Böker, T., Falcón-Barroso, J., Schinnerer, E., Knapen, J. H., & Ryder, S. 2008, AJ, 135, 479
Comerón, S., Knapen, J. H., & Beckman, J. E. 2008, A&A, 485, 695
Dale, D. A., & Helou, G. 2002, ApJ, 576, 159
Dale, D. A., et al. 2007, ApJ, 655, 863
Dale, D. A., et al. 2009, ApJ, 703, 517
Draine, B. T., et al. 2007, ApJ, 663, 866
Draine, B. T., & Li, A. 2007, ApJ, 657, 810
Dunne, L., Eales, S., Edmunds, M., Ivison, R., Alexander, P., & Clements, D. L. 2000, MNRAS, 315, 115
Dunne, L., & Eales, S. A. 2001, MNRAS, 327, 697
Dupac, X., et al. 2003, MNRAS, 344, 105
Engelbracht, C. W., Rieke, G. H., Gordon, K. D., Smith, J.-D. T., Werner, M. W., Moustakas, J., Willmer, C. N. A., & Vanzi, L. 2008, ApJ, 678, 804
Erwin, P., & Sparke, L. S. 2002, AJ, 124, 65
Gordon, K. D., et al. 2007, PASP, 119, 1019
Gordon, K. D., Engelbracht, C. W., Rieke, G. H., Misselt, K. A., Smith, J.-D. T., & Kennicutt, R. C., Jr. 2008, ApJ, 682, 336
Griffin, et al. 2010, this volume
Hauser, M. G., & Dwek, E. 2001, ARA&A, 39, 249
Hawarden, T. G., Mountain, C. M., Leggett, S. K., & Puxley, P. J. 1986, MNRAS, 221, 41P
Ho, L. C., Filippenko, A. V., & Sargent, W. L. W., 1997, ApJS, 112, 315
Huang, J. H., Gu, Q. S., Su, H. J., Hawarden, T. G., Liao, X. H., & Wu, G. X. 1996, A&A, 313, 13
Hunt, L. K., & Malkan, M. A. 1999, ApJ, 516, 660
Kennicutt, R. C., Jr., et al. 2003, PASP, 115, 928
Knapen, J. H. 2005, A&A, 429, 141
Koda, J., Okuda, T., Nakanishi, K., Kohno, K., Ishizuki, S., Kuno, N., & Okumura, S. K. 2005, A&A, 431, 887
Liu, G., et al. 2010, AJ, 139, 1190
Masters, K. L., et al. 2010, arXiv:1003.0449
Melo, V. P., Pérez García, A. M., Acosta-Pulido, J. A., Muñoz-Tuñón, C., & Rodríguez Espinosa, J. M. 2002, ApJ, 574, 709
Muñoz-Mateos, J. C., et al. 2009, ApJ, 701, 1965
Ott, S. 2010, in ASP Conference Series, Astronomical Data Analysis Software and Systems XIX, Y. Mizumoto, K.-I. Morita, and M. Ohishi, eds., in press
Pilbratt, et al. 2010, this volume
Poglitsch, et al. 2010, this volume
Popescu, C. C., Misiriotis, A., Kylafis, N. D., Tuffs, R. J., & Fischera, J. 2000, A&A, 362, 138
Radovich, M., Kahanpää, J., & Lemke, D. 2001, A&A, 377, 73
Rieke, G. H., et al. 2004, ApJS, 154, 25
Roussel, H., et al. 2001, A&A, 372, 406

Sakamoto, K., Okumura, S. K., Ishizuki, S., & Scoville, N. Z. 1999, ApJ, 525, 691

Sandstrom, et al. 2010, this volume

Seaquist, E., Yao, L., Dunne, L., & Cameron, H. 2004, MNRAS, 349, 1428

Siebenmorgen, R., Krügel, E., & Chini, R. 1999, A&A, 351, 495

Stansberry, J. A., et al. 2007, PASP, 119, 1038

Stevens, J. A., Amure, M., & Gear, W. K. 2005, MNRAS, 357, 361

Swinyard, B. M., Ade, P., Baluteau, J-P., et al. 2010, this volume

Vlahakis, C., Dunne, L., & Eales, S. 2005, MNRAS, 364, 1253

Willmer, C. N. A., Rieke, G. H., Le Floc'h, E., Hinz, J. L., Engelbracht, C. W., Marcillac, D., & Gordon, K. D. 2009, AJ, 138, 146

[1] Steward Observatory, University of Arizona, Tucson, AZ 85721, USA
e-mail: cengelbracht@as.arizona.edu

[2] INAF - Osservatorio Astrofisico di Arcetri, Largo E. Fermi 5, 50125 Firenze, Italy

[3] Department of Astronomy, University of Massachusetts, Amherst, MA 01003, USA

[4] Space Telescope Science Institute, 3700 San Martin Drive, Baltimore, MD 21218, USA

[5] Institut d'Astrophysique de Paris, UMR7095 CNRS, Université Pierre & Marie Curie, 98 bis Boulevard Arago, 75014 Paris, France

[6] Department of Astronomy, University of Maryland, College Park, MD 20742, USA

[7] Institute of Astronomy, University of Cambridge, Madingley Road, Cambridge CB3 0HA, UK

[8] NASA Herschel Science Center, IPAC, California Institute of Technology, Pasadena, CA 91125, USA

[9] Spitzer Science Center, California Institute of Technology, MC 314-6, Pasadena, CA 91125, USA

[10] Leiden Observatory, Leiden University, P.O. Box 9513, 2300 RA Leiden, The Netherlands

[11] Department of Physics and Astronomy, University of Toledo, 2801 West Bancroft Street, Toledo, OH 43606, USA

[12] Department of Physics & Astronomy, University of Wyoming, Laramie, WY 82071, USA

[13] Department of Astrophysical Sciences, Princeton University, Princeton, NJ 08544, USA

[14] Max-Planck-Institut für Astronomie, Königstuhl 17, 69117 Heidelberg, Germany

[15] Departamento de Astrofisica, Facultad de Ciencias Fisicas, Universidad Complutense Madrid, Ciudad Universitaria, Madrid, E-28040, Spain

[16] Tianjin Astrophysics Center, Tianjin Normal University, Tianjin 300387, China

[17] Department of Physics and Astronomy, SUNY Stony Brook, Stony Brook, NY 11794-3800, USA

[18] National Radio Astronomy Observatory, 520 Edgemont Road, Charlottesville, VA 22903, USA

[19] Department of Physics & Astronomy, McMaster University, Hamilton, Ontario L8S 4M1, Canada

[20] CEA/DSM/Irfu/Service d'Astrophysique, UMR AIM, CE Saclay, 91191 Gif sur Yvette Cedex, France

[21] ICRAR, M468, University of Western Australia, 35 Stirling Hwy, Crawley, WA, 6009, Australia